

*Experimental*

Colloidal gold nanorods with an aspect ratio of 2.9 (width  $12 \pm 2$  nm) were synthesized by a modified version of the seed-growth method [22] developed by Jana and co-workers [23]. The seed solution consisted of 5 ml of 0.2 M cetyltrimethylammonium bromide (CTAB) solution mixed with 5 ml of 0.0005 M  $\text{HAuCl}_4$ . To the stirred solution, 0.6 ml of ice-cold 0.01 M  $\text{NaBH}_4$  was added. Vigorous stirring of the seed solution was continued for 2 min. After stirring, the solution was kept at 25 °C. The growth solution was prepared with 5 ml of 0.2 M CTAB added to 0.1 ml of 0.004 M  $\text{AgNO}_3$  solution. To this solution 5 ml of 0.001 M  $\text{HAuCl}_4$  was added, and after gentle mixing of the solution, 70  $\mu\text{L}$  of 0.0788 M ascorbic acid was added. In the final step, 12  $\mu\text{L}$  of the seed solution was added to the growth solution. The size of the gold nanorods were determined using transmission electron microscopy (TEM).

Regular arrays of gold nanoparticles were prepared using nanosphere lithography following the method developed by van Duyne and co-workers [12,13]. An ordered layer of 356 nm polystyrene nanospheres (Polysciences) was prepared on a glass coverslip (Fisher Scientific). The coverslips were mounted in a Denton DV-502A Thermal Evaporator to deposit gold in the spaces between the spheres. The thickness of the evaporated gold was monitored by a quartz crystal thickness monitor (Inficon). After evaporation, the mask was removed from the substrate by sonicating for 30 s in methylene chloride. The size of the particles is determined by the polystyrene mask and was 90 nm wide at its base and 50 nm in height in these studies, as verified using a Quesant Q-SCOPE atomic force microscope (AFM).

Absorption spectra were recorded using a Shimadzu UV-3101-PC spectrophotometer. Transient absorption studies [18,19] were performed using an amplified Ti:Sapphire laser system (Clark CPA 100). The second harmonic of the 800 nm fundamental was used as excitation and a white-light continuum probe beam was generated by focusing a small part of the fundamental beam into a sapphire window. The pump beam was mechanically chopped and the differential transmission signal was recorded using a pair of Si photodiodes (Thorlab) and a lock-in amplifier (Stanford Research Systems).

Received: October 9, 2002

**“Beaded” Bimetallic Nanowires: Wiring Nanoparticles of Metal 1 Using Nanowires of Metal 2\*\***

By *Erich C. Walter, Benjamin J. Murray, Fred Favier, and Reginald M. Penner\**

Bimetallic nanowires that are compositionally modulated along the axis of the nanowire can form the basis for nanowire-based devices including diodes,<sup>[1–3]</sup> spin valves,<sup>[4–8]</sup> and optical labels (“Nanobar codes”).<sup>[9–11]</sup> One convenient method for preparing such nanowires is using template synthesis<sup>[12–14]</sup> which involves the electrodeposition of a metal into the uniform cylindrical<sup>[13–15]</sup> or prismatic<sup>[16]</sup> pores of a host membrane. In a template synthesis experiment, layered nanowires are obtained by halting the electrodeposition of one metal, changing the plating solution for one containing a different metal ion, and resuming deposition.<sup>[8]</sup> This approach allows precise control over the composition and thickness of the individual metal layers within the nanowire, as well as the nanowire diameter. However, using template synthesis limits the total length of a nanowire to 20  $\mu\text{m}$  or so.

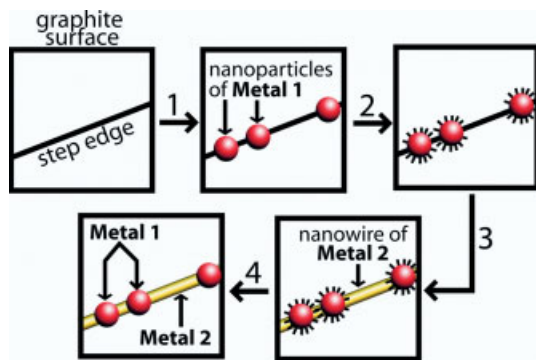
Here, we describe a second, complimentary method for preparing long ( $> 100 \mu\text{m}$ ) bimetallic nanowires that are compositionally modulated along the axis of the nanowire. Essentially, the new method described here involves “wiring” together particles of one metal using nanowires of a second. This is accomplished by combining two new electrodeposition methods that we have recently described: “Slow growth” for preparing metal nanoparticles that are narrowly dispersed in diameter,<sup>[17–19]</sup> and nanowire growth.<sup>[19–21]</sup> Using this approach, beaded bimetallic nanowires that are up to a millimeter in length can be prepared in parallel arrays on a graphite surface. These wires can then be transferred onto a second, insulating surface, e.g., glass, using a method we have previously described.<sup>[22]</sup>

The procedure for preparing beaded, bimetallic nanowires is summarized in Scheme 1. First, nanoparticles of “metal 1” (copper, nickel, silver, gold, palladium, or platinum) were electrodeposited onto a highly oriented pyrolytic graphite surface. Using specified “slow growth” conditions,<sup>[17,18]</sup> metal particles nucleated preferentially at step edges present on this surface. These particles were then covered with an organic self-assembled monolayer (SAM) by exposing them to an eth-

[1] a) J. Yguerabide, E. E. Yguerabide, *Anal. Biochem.* **1998**, *262*, 137. b) J. Yguerabide, E. E. Yguerabide, *Anal. Biochem.* **1998**, *262*, 157.  
 [2] K. Hamad-Schifferli, J. J. Schwartz, A. T. Santos, S. Zhang, J. M. Jacobson, *Nature* **2002**, *415*, 152.  
 [3] M. A. El-Sayed, *Acc. Chem. Res.* **2001**, *34*, 257.  
 [4] S. Link, C. Burda, M. B. Mohamed, B. Nikoobakht, M. A. El-Sayed, *J. Phys. Chem. A* **1999**, *103*, 1165.  
 [5] H. Kurita, A. Takami, S. Koda, *Appl. Phys. Lett.* **1998**, *72*, 789.  
 [6] F. Mafune, J. Kohno, Y. Takeda, T. Kondow, *J. Phys. Chem. B* **2002**, *106*, 7575.  
 [7] S. Link, M. A. El-Sayed, *J. Phys. Chem. B* **1999**, *103*, 8410.  
 [8] R. Gans, *Ann. Phys.* **1915**, *47*, 270.  
 [9] M. Maillard, S. Giorgio, M. P. Pileni, *Adv. Mater.* **2002**, *14*, 1084.  
 [10] R. Jin, Y. W. Cao, C. A. Mirkin, K. L. Kelly, G. C. Schatz, J. G. Zheng, *Science* **2001**, *294*, 1901.  
 [11] T. R. Jensen, G. C. Schatz, R. P. Van Duyne, *J. Phys. Chem. B* **1999**, *103*, 2394.  
 [12] C. L. Haynes, R. P. Van Duyne, *J. Phys. Chem. B* **2001**, *105*, 5599.  
 [13] C. L. Haynes, A. D. McFarland, M. T. Smith, J. C. Hulteen, R. P. Van Duyne, *J. Phys. Chem. B* **2002**, *106*, 1898.  
 [14] C. Voisin, N. Del Fatti, D. Christofilos, F. Vallee, *J. Phys. Chem. B* **2001**, *105*, 2264.  
 [15] a) J. H. Hodak, A. Henglein, G. V. Hartland, *J. Phys. Chem. B* **2000**, *104*, 9954. b) C. L. Haynes, A. D. McFarland, M. T. Smith, J. C. Hulteen, R. P. Van Duyne, *Phys. Chem. B* **2002**, *106*, 1898.  
 [16] M. Perner, P. Bost, G. von Plessen, J. Feldmann, U. Becker, M. Mennig, H. Schmidt, *Phys. Rev. Lett.* **1997**, *78*, 2192.  
 [17] M. Hu, G. V. Hartland, *J. Phys. Chem. B* **2002**, *106*, 7029.  
 [18] S. Link, A. Furube, M. B. Mohamed, T. Asahi, H. Masuhara, M. A. El-Sayed, *J. Phys. Chem. B* **2002**, *106*, 945.  
 [19] M. B. Mohamed, T. S. Ahmadi, S. Link, M. Braun, M. A. El-Sayed, *Chem. Phys. Lett.* **2001**, *343*, 55.  
 [20] V. Halte, J.-Y. Bigot, B. Palpant, M. Broyer, B. Prevel, A. Perez, *Appl. Phys. Lett.* **1999**, *75*, 3799.  
 [21] S. L. Westcott, R. D. Averitt, J. A. Wolfgang, P. Nordlander, N. J. Halas, *J. Phys. Chem. B* **2001**, *105*, 9913.  
 [22] B. Nikoobakht, M. A. El-Sayed, unpublished.  
 [23] N. R. Jana, L. Gearheart, C. J. Murphy, *J. Phys. Chem. B* **2001**, *105*, 4065.

[\*] Prof. R. M. Penner, E. C. Walter, B. J. Murray  
 Institute for Surface and Interface Science  
 Department of Chemistry, University of California, Irvine  
 Irvine, CA 92679-2025 (USA)  
 E-mail: rmpenner@uci.edu  
 Dr. F. Favier  
 UMR 5072 CNRS - UMII  
 F-34095 Montpellier (France)

[\*\*] This work was funded by the National Science Foundation (#CHE-0111557 and INT 0233371). R. P. acknowledges the financial support of the A. P. Sloan Foundation Fellowship, and the Camille and Henry Dreyfus Foundation. F. F. acknowledges funding through NATO. Finally, donations of graphite by Dr. Art Moore of Advanced Ceramics are gratefully acknowledged.



Scheme 1. Schematic diagram illustrating the preparation of beaded, bimetallic nanowires using electrochemical step-edge decoration. The steps involved are: 1) Nanoparticles of Metal 1 are electrodeposited from an aqueous plating solution using the “slow growth” method described previously. The nucleation of these particles occurs preferentially at step edges present on the graphite surface, as shown. 2) The surface is rinsed with water, and exposed to a solution containing an *n*-alkanethiol (heavy lines). A monolayer of the thiol self-assembles on the surface of the particles of Metal 1. 3) The surface is rinsed with ethanol, immersed in a second plating solution, and nanowires of Metal 2 are electrodeposited as previously described. During this process, the presence of the *n*-alkanethiol monolayer prevents electrodeposition onto the particles of Metal 1. 4) Finally, if necessary the *n*-alkanethiol monolayer is thermally removed from Metal 1 by heating the surface for an hour in hydrogen at 500 °C.

anolic solution of *n*-hexanethiol. This organic monolayer electrically insulated the metal particles from contact with a metal plating electrolyte solution.<sup>[23]</sup> Finally, nanowires of “metal 2” (copper, iron, palladium)<sup>[19,21,23]</sup> or a conductive metal oxide (MoO<sub>2</sub>)<sup>[20,24]</sup> were electrodeposited using the electrochemical step-edge decoration (ESED) method. As shown in Scheme 1, nanowire growth occurred preferentially at step edges that were not blocked by particles of metal 1. In this process, the pre-existing particles of metal 1 located at step edges were linked by nanowire segments of metal 2.

Scanning electron microscopy (SEM) images obtained at three junctures during the preparation of the silver particles/copper nanowires bimetallic system are shown in Figure 1. Figure 1a shows the graphite electrode surface after the electrodeposition of silver nanoparticles. Silver particles nucleate preferentially along two step edges present in this region of the graphite surface. These silver particles were then exposed to the *n*-hexanethiol solution overnight, the surface was rinsed with ethanol, and immersed in a copper plating solution (Table 1). Copper nanowires were then electrodeposited as previously described.<sup>[21]</sup> Formation of a copper nanowire occurred everywhere along step edges except where silver particles blocked deposition. The result, shown in Figure 1b, was silver particles connected together with copper nanowires. From this SEM image, it is impossible to determine the extent to which silver and copper segments of these bimetallic nanowires are bonded to one another. However it was routinely possible to transfer bimetallic nanowires off of the graphite surface by embedding these nanostructures in epoxy as previously described.<sup>[22]</sup> Figure 1c shows the beaded nanowires on the epoxy surface after this transfer was carried out. The surface of the nanowires seen in this image was in contact with the graphite surface during growth and the imprint of the step

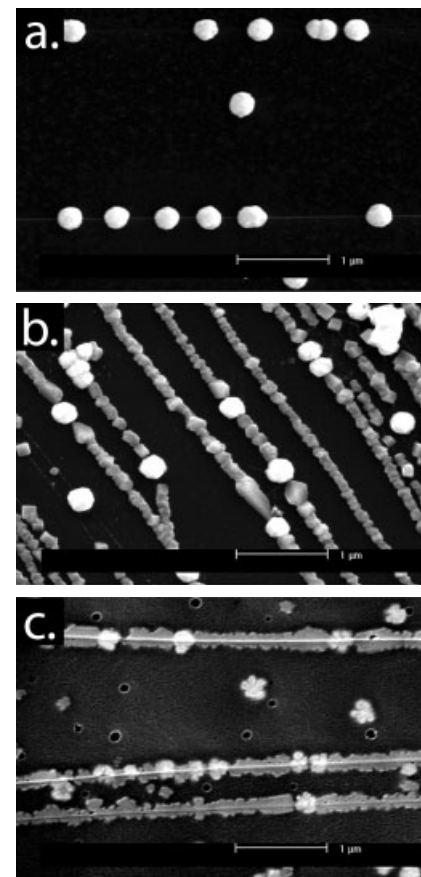


Fig. 1. Scanning electron microscopy images obtained at three junctures during the preparation of bimetallic nanowires with silver particles and copper connecting segments. a) Image of a graphite surface after the electrodeposition of silver particles using a “slow growth” protocol. These particles form preferentially at step edges on the graphite surface. b) Image acquired after self-assembly of the *n*-hexanethiol capping layer, and the electrodeposition of a copper nanowire using conditions summarized in Table 1. c) Image acquired after embedding the bimetallic nanowire in epoxy and transfer to a glass surface. In this image, the surface of the nanowire that was originally in contact with the graphite surface is seen. The imprint of the step edge along the axis of each nanowire is clearly visible.

Table 1. Source and purity of the metal salts and electrolytes employed for nanowire growth.

	Plating solution	Purity, Source [a]
Ag	Ag <sub>2</sub> SO <sub>4</sub>	C, F
	saccharine	98+%, A
Fe	Na <sub>2</sub> SO <sub>4</sub>	C, F
	FeSO <sub>4</sub> · 7 H <sub>2</sub> O	C, F
	H <sub>2</sub> SO <sub>4</sub>	C, F
Mo	Na <sub>2</sub> MoO <sub>4</sub>	98+%, A
	NaCl	C, F
Pd	NH <sub>4</sub> Cl	R, F
	Pd(NO <sub>3</sub> ) <sub>2</sub>	R, F
	HClO <sub>4</sub>	R, F
Pt	H <sub>2</sub> PtCl <sub>6</sub>	99.99%, A
	HCl	R, F
Cu	CuSO <sub>4</sub> · 5H <sub>2</sub> O	99.999%, AA
	Na <sub>2</sub> SO <sub>4</sub>	C, F
Au	AuCl <sub>3</sub>	99.99+%, A
	NaCl	C, F

C: certified ACS, R: reagent grade, A: Aldrich, F: Fischer, AA: AlfaAesar

edge along the axis of the nanowire is clearly visible. The vast majority (>80%) of nanowires survive this transfer process without breaking. This suggests that a good mechanical bond exists between metal 1 and metal 2.

During the step-wise assembly of beaded, bimetallic nanowires the *n*-hexanethiol layer prevents the electrodeposition of metal 2 atop the particles of metal 1. Confirmation of this fact is obtained by energy-dispersive X-ray (EDX) elemental mapping of the nanowires after wire deposition. In Figure 2, for example, an elemental map of the silver particle/copper

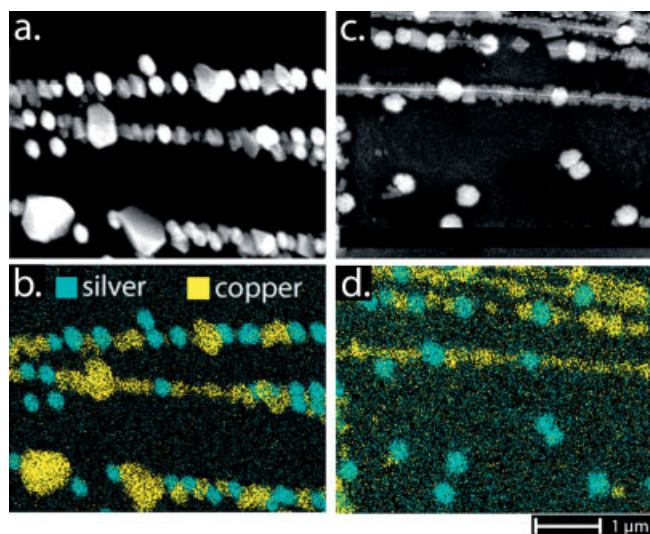


Fig. 2. a,c) Scanning electron microscopy images and b,d) corresponding energy-dispersive X-ray elemental maps for copper/silver bimetallic nanowires. a,b) Bimetallic nanowires with silver particles and copper connecting segments after synthesis on a graphite surface. c,d) The same nanowires after embedding in epoxy and transfer to a glass surface. The surface of this sample was sputter-coated with several nanometers of gold-palladium to eliminate charging effects. Collectively, these two elemental maps which show the same nanowires from opposite sides proves that the silver nanoparticles are disposed in series with the copper nanowires; the copper nanowires do not “shunt” these silver particles.

wire of Figure 2a is shown in Figure 2b. The silver (blue) and copper (yellow) domains of this wire are cleanly delineated.

As already indicated, the bimetallic nanowires prepared here are “portable”: These nanowires can be transferred from the graphite surface on which they are synthesized onto a second surface. Figure 2c shows a silver particle/copper nanowire after embedding in epoxy and transfer to a glass surface. Again, copper and silver domains are cleanly delineated within the embedded nanowire. The portability of these bimetallic nanowires facilitates their incorporation into devices such as sensors.<sup>[22,25,26]</sup> These data also indicate that silver particles are connected *in series* with the copper nanowire. In other words, the EDX maps demonstrate that a copper layer does not grow either beneath the silver particles on the graphite surface (Fig. 2d) or on top of these particles (Fig. 2b).

The method described here can be used to prepare a variety of bimetallic nanowire systems. The key constraints of the method are the following: 1) A compact self-assembled monolayer of an *n*-hexanethiol monolayer must form atop particles of metal 1. This means metal 1 must be a coinage or noble

metal. 2) Metal 1 must be more noble than metal 2. In other words, the deposition potential for metal 1 must be more positive than that of metal 2. If this is not the case, then particles of metal 1 will dissolve as nanowires of metal 2 are electrodeposited. We have found that this dissolution occurs to a significant extent when these particles are covered with a monolayer of *n*-hexanethiol. 3) A procedure for forming nanowires of metal 2 must exist.

Because the separate methods for preparing metal particles and metal nanowires are both extremely general, the combination of these two methods can be used to prepare a wide variety of metal particle/metal nanowire bimetallic systems. SEM images of ten different systems are shown in Figure 3.

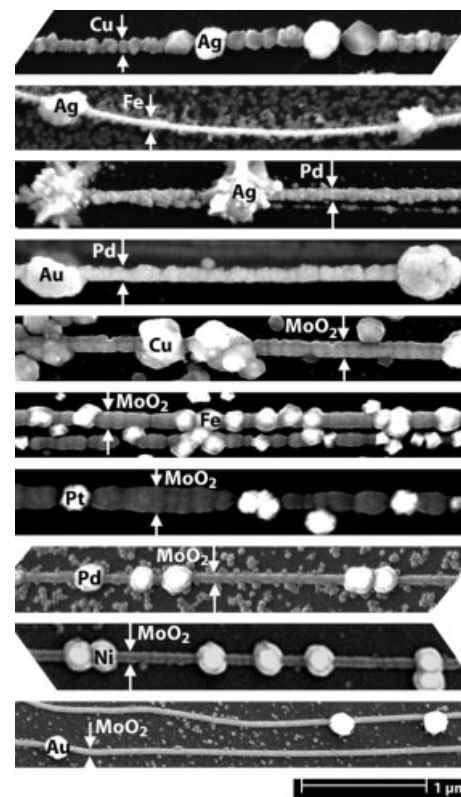


Fig. 3. Scanning electron microscopy images of ten bimetallic particle/wire systems.

In summary, metal nanoparticle/metal nanowire bimetallic systems have been prepared by growing nanowires along an axis connecting a series of nanoparticles aligned at the step edge of a graphite surface. The method described has two disadvantages relative to template synthesis. First, metal particles are randomly distributed along the axis of a nanowire, and, second, all of these particles are of equal diameter. Adjustability of the particle diameter and location along the nanowire can not be achieved. However, the method described here also possesses three advantages. First, as already indicated, extremely long nanowires can be prepared. Secondly, the diameter of the metal particles and that of the nanowire can be independently specified during growth. Finally, the synthesis of bimetallic nanowires is a parallel process: all particles of metal

1 are deposited in a single operation; nanowire growth is likewise one step.

## Experimental

**Electrochemical Synthesis:** The electrodeposition of metal particles and wires onto freshly cleaved highly oriented pyrolytic graphite (HOPG) occurred in a 50 mL, one compartment, glass and Teflon cell. A 0.14 cm<sup>2</sup> circular area of the basal plane of HOPG was isolated as the working electrode using an o-ring in a Teflon electrode holder. Reference electrodes appropriate to each plating solution were employed, but in the text all potentials are referenced to the saturated calomel electrode. A 2 cm<sup>2</sup> Pt foil functioned as the counter electrode in these experiments.

Particles and wires were deposited out of N<sub>2</sub>-purged solutions prepared with Barnstead Nanopure water ( $\rho > 17.8 \text{ M}\Omega$ ). The source and purity of metal salts and electrolytes are summarized in Table 1. Nanowires and nanoparticles were grown according to previously reported methods. For each system, the synthesis conditions are summarized in Table 2. Previously unreported iron nanowires were prepared by applying a 5 ms nucleation pulse of  $-2 \text{ V}$  vs Fe wire followed by a growth pulse of  $-1 \text{ V}$  for 120 s. All electrodepositions were performed using

computer-controlled potentiostats from EG&G Princeton Applied Research (models: 273 A, 263 A, Versastat).

**Self-Assembled Monolayer:** Metal particles were encapsulated in a self-assembled monolayer of *n*-hexanethiol by soaking in 1 mM *n*-hexanethiol (95+ % Aldrich) in EtOH (200 Proof, Gold Shield) overnight [25]. Samples were subsequently rinsed with EtOH prior to deposition of wires.

**Transfer of Nanowires:** The surface of the graphite electrode onto which nanowires had been deposited was pressed onto a droplet ( $\approx 50 \mu\text{L}$ ) of cyanoacrylate adhesive ("Special T" super glue, Satellite City) on a degreased glass slide. After this adhesive hardened, the graphite surface was lifted off the cyanoacrylate, and residual carbon layers were removed with a forceps. In general, more than 80 % of the nanowires initially present on the graphite surface were transferred onto the surface of the cyanoacrylate film using this procedure.

**Characterization:** Scanning electron microscopy (SEM) images and energy-dispersive X-ray (EDX) analysis were acquired on a Philips Model XL-30FEG operating at 10–30 keV. Samples were mounted on aluminum SEM stubs using adhesive carbon dots (Ted Pella).

Received: October 9, 2002

Table 2. Plating potentials and plating solution compositions employed for the preparation of beaded bimetallic nanowires shown in Figures 1–3.

Composition of particles	Composition of wires	Plating conditions for particles	Plating conditions for wires
silver	copper	1.3 mM AgSO <sub>4</sub> 1.2 mM saccharine 15 ms $\times$ $-1.0 \text{ V}$ + 60s $\times$ $-200 \text{ mV}$ vs. Ag wire	2.0 mM CuSO <sub>4</sub> ·5H <sub>2</sub> O 0.1 M Na <sub>2</sub> SO <sub>4</sub> 5 ms $\times$ $-800 \text{ mV}$ + 1200 s $\times$ $-5 \text{ mV}$ vs. Cu wire
silver	iron	same	12 mM FeSO <sub>4</sub> 0.5 M Na <sub>2</sub> SO <sub>4</sub> H <sub>2</sub> SO <sub>4</sub> $\sim$ 15 drops 5 ms $\times$ $-2 \text{ V}$ + 120 s $\times$ $-1 \text{ V}$ vs. Fe wire
silver	palladium	same	1.5 mM PdCl <sub>2</sub> 0.1 M HCl 5 ms $\times$ $-250 \text{ mV}$ + 2700 $\times$ 350 mV vs. SCE
copper	MoO <sub>2</sub>	2.0 mM CuSO <sub>4</sub> ·5H <sub>2</sub> O 0.1 M Na <sub>2</sub> SO <sub>4</sub> 5 ms $\times$ $-800 \text{ mV}$ + 100 s $\times$ $-100 \text{ mV}$	10 mM Na <sub>2</sub> MoO <sub>4</sub> 1.0 M NaCl 1.0 M NH <sub>4</sub> Cl 70 s $\times$ $-875 \text{ mV}$ vs. SCE
iron	MoO <sub>2</sub>	12 mM FeSO <sub>4</sub> 0.5 M Na <sub>2</sub> SO <sub>4</sub> H <sub>2</sub> SO <sub>4</sub> $\sim$ 15 drops 5 ms $\times$ $-2 \text{ V}$ + 10 s $\times$ $-1 \text{ V}$ vs. Fe wire	same
platinum	MoO <sub>2</sub>	1.5 mM H <sub>2</sub> PtCl <sub>6</sub> 0.1 M HCl 5 ms $\times$ $-300 \text{ mV}$ + 60 s $\times$ $-150 \text{ mV}$ vs. SCE	same
palladium	MoO <sub>2</sub>	1.5 mM PdCl <sub>2</sub> 0.1 M HCl 5 ms $\times$ $-450 \text{ mV}$ + 60 s $\times$ 350 mV vs. SCE	same
nickel	MoO <sub>2</sub>	2.0 mM NiCl <sub>2</sub> 0.2 M NaCl 5 ms $\times$ $-1.0 \text{ mV}$ + 60 s $\times$ $-800 \text{ mV}$ vs. SCE	same
gold	MoO <sub>2</sub>	1.0 mM AuCl <sub>3</sub> 0.1 M NaCl 5 ms $\times$ 200 mV + 10 s $\times$ 500 mV vs. SCE.	same

- J. K. N. Mbindyo, T. E. Mallouk, J. B. Mattzela, I. Kratochvilova, B. Razavi, T. N. Jackson, T. S. Mayer, *J. Am. Chem. Soc.* **2002**, *124*, 4020.
- N. I. Kovtyukhova, B. R. Martin, J. K. N. Mbindyo, T. E. Mallouk, M. Cabassi, T. S. Mayer, *Mater. Sci. Eng. C* **2002**, *19*, 255.
- N. I. Kovtyukhova, B. R. Martin, J. K. N. Mbindyo, P. A. Smith, B. Razavi, T. S. Mayer, T. E. Mallouk, *J. Phys. Chem. B* **2001**, *105*, 8762.
- B. Doudin, J. E. Wegrowe, S. E. Gilbert, V. Scarni, D. Kelly, J. P. Meier, J. P. Ansermet, *IEEE Trans. Magn.* **1998**, *34*, 968.
- A. Blondel, J. P. Meier, B. Doudin, J. P. Ansermet, *Appl. Phys. Lett.* **1994**, *65*, 3019.
- B. Doudin, A. Blondel, J. P. Ansermet, *J. Appl. Phys.* **1996**, *79*, 6090.
- G. P. Heydon, S. R. Hoon, A. N. Farley, S. L. Tomlinson, M. S. Valera, K. Attenborough, W. Schwarzscher, *J. Phys. D: Appl. Phys.* **1997**, *30*, 1083.
- K. Liu, K. Nagodawithana, P. C. Searson, C. L. Chien, *Phys. Rev. B* **1995**, *51*, 7381.
- S. R. Nicewarner-Pena, R. G. Freeman, B. D. Reiss, L. He, D. J. Pena, I. D. Walton, R. Cromer, C. D. Keating, M. J. Natan, *Science* **2001**, *294*, 137.
- I. D. Walton, S. M. Norton, A. Balasingham, L. He, D. F. Oviso, D. Gupta, P. A. Raju, M. J. Natan, R. G. Freeman, *Anal. Chem.* **2002**, *74*, 2240.
- B. D. Reiss, R. G. Freeman, I. D. Walton, S. M. Norton, P. C. Smith, W. G. Stonas, C. D. Keating, M. J. Natan, *J. Electroanal. Chem.* **2002**, *522*, 95.
- J. C. Hulteen, C. R. Martin, *J. Mater. Chem.* **1997**, *7*, 1075.
- C. R. Martin, *Science* **1994**, *266*, 1961.
- C. R. Martin, *Chem. Mater.* **1996**, *8*, 1739.
- C. A. Foss, M. J. Tierney, C. R. Martin, *J. Phys. Chem.* **1992**, *96*, 9001.
- T. M. Whitney, J. S. Jiang, P. C. Searson, C. L. Chien, *Science* **1993**, *261*, 1316.
- H. Liu, R. M. Penner, *J. Phys. Chem. B* **2000**, *104*, 9131.
- H. Liu, F. Favier, K. Ng, M. P. Zach, R. M. Penner, *Electrochim. Acta* **2001**, *47*, 671.
- R. M. Penner, *J. Phys. Chem. B* **2002**, *106*, 3339.
- M. P. Zach, K. H. Ng, R. M. Penner, *Science* **2000**, *290*, 2120.
- E. Walter, B. Murray, F. Favier, G. Kaltenpoth, M. Grunze, R. M. Penner, *J. Phys. Chem. B* **2002**, *106*, 11407.
- E. C. Walter, F. Favier, R. M. Penner, *Anal. Chem.* **2002**, *74*, 1546.
- W. Li, J. A. Virtanen, R. M. Penner, *J. Phys. Chem.* **1994**, *117*, 751.
- M. P. Zach, K. Inazu, J. C. Hemminger, R. M. Penner, *Chem. Mater.* **2002**, *14*, 3206.
- K. H. Ng, R. M. Penner, *J. Electroanal. Chem.* **2002**, *522*, 86.
- F. Favier, E. Walter, M. P. Zach, T. Benter, R. M. Penner, *Science* **2001**, *293*, 2227.